Catalysis Today 139 (2008) 140–145

Contents lists available at ScienceDirect

Catalysis Today

journal homepage: www.elsevier.com/locate/cattod

Promotion effect of Al_2O_3–SiO_2 interlayer and Pt loading on TiO_2/nickel-foam photocatalyst for degrading gaseous acetaldehyde

Jian Yuan, Hai Hu, Mingxia Chen, Jianwei Shi, Wenfeng Shangguan *

Research Center for Combustion and Environment Technology, Shanghai Jiao Tong University, Shanghai 200240, PR China

ARTICLE INFO

Article history:
Available online 16 September 2008

Keywords:
Photocatalysis
Foam nickel
TiO_2
Interlayer
Pt loading
Acetaldehyde degradation

ABSTRACT

TiO_2 photocatalysts coated on foam nickel were prepared by sol–gel method. Al_2O_3–SiO_2 films introducing as transition interlayer between TiO_2 and nickel metal foam were used to promote the photocatalytic activity of TiO_2. The results show that TiO_2/Al_2O_3–SiO_2 composite films have much higher photocatalytic activity and stability for degradation of gaseous acetaldehyde than TiO_2 films. The significant enhancement effect arises from the large specific surface area of Al_2O_3–SiO_2, which provides more active sites for subsequent TiO_2 loading and photocatalytic reaction. The Al_2O_3–SiO_2 interlayer also inhibits the transfer of photo-generated electron from TiO_2 to Ni metal and improves the photocatalytic activity of photocatalysts. Furthermore, Pt loading on TiO_2 by photo-deposition was carried out to improve photocatalytic efficiency. The acetaldehyde degradation rate on Pt-loaded TiO_2 photocatalyst is more than three times than that of TiO_2 without Pt loading. The optimum Pt concentration is 0.3 wt%. XRD, UV–vis and SEM were used to characterize the structural, physical and chemical features of all the samples and to reveal the mechanism of the improvement of the photocatalytic activity. The effects of photocatalyst preparation parameters along with their photocatalytic behavior in deactivation and reactivation are also presented in the present study.

1. Introduction

In recent years, photocatalytic degradation of various kinds of organic pollutants using semiconductor TiO_2 as photocatalyst has been extensively studied. Since the organic pollutants could be completely decomposed into CO_2 and H_2O, photocatalytic method should be one of the most effective means in dealing with the problem of environmental pollution [1–3].

The effective removal of volatile organic compounds (VOCs) by photocatalytic technique has become the focus in the field of indoor air quality (IAQ) [4,5]. However, the photo-degradation efficiency is still very low because the concentration of indoor pollutants is usually at ppmv level. The lower pollutant concentration results in lower photocatalytic reaction rate. Moreover, the recombination of photo-generated charge carrier occurs within nanoseconds, leading to limited photoactivity of TiO_2.

Most of the studies about the photocatalysts of TiO_2 are focused on powder TiO_2. For gaseous photocatalytic applications, there exists tough problem of TiO_2 immobilization on solid substrate. Film-type photocatalysts normally have lower surface areas than powder ones. However, the decrease of surface area might seriously impair the photocatalytic activity of TiO_2. On the other hand, the interaction between TiO_2 film and the surface of different substrates could also have different effects on the photocatalytic process. It is reported that many approaches have been taken to prepare immobilized photocatalysts [6,7] on various supports, such as magnetron-sputtering [8], chemical vapor deposition [9] and sol–gel process [10]. Some highly porous materials were chosen as catalyst supports, such as ceramic foam [11–13], porous alumina [14,15], porous silica [16], zeolite [17], activated carbon [18], etc. The results presented that the combination of TiO_2 and supports with high specific surface area or high adsorbability were effective for improving of photo-decomposition rate.

Foam nickel, which provides the catalytic system excellent gas-dynamic properties and sufficient contact of the gaseous reactants with the catalyst surface due to its uniform open-porous and reticulate structure, has been used as a support of TiO_2 photocatalyst by sol–gel process in our previous works. It showed that increment of specific surface area (SSA) of foam nickel by pre-heating treatment resulted in the enhancement of photocatalytic activity [19]. The pre-heating for foam nickel substrates made the formation of NiO layer, which prevented effectively the injection of photo-generated electrons from TiO_2 films to metal Ni. Since the SSA of foam nickel is still very low, the modification of foam nickel

* Corresponding author. Fax: +86 21 34206020.
E-mail address: shangguan@sjtu.edu.cn (W. Shangguan).

0920-5861/$ – see front matter © 2008 Elsevier B.V. All rights reserved.
doi:10.1016/j.cattod.2008.08.016

aiming to increase its SSA is feasible to be developed. In the present work, Al_2O_3–SiO_2 films were prepared as interlayer between TiO_2 and foam nickel by sol–gel method. Usually, the binary sol of Al_2O_3–SiO_2 is easy to be synthesized, and alumina–silicate has good chemical durability and mechanical properties.

Attempts have primarily been made to improve the photocatalytic efficiency of TiO_2 by doping metals [20–22]. The doped metal with high electron affinity effectively traps the photo-excited electrons and utilizes them to perform subsequent reduction reaction. In addition, the holes participate in the oxidation reaction, thereby increasing the overall efficiency of the process [23]. In this paper, platinized TiO_2 films were prepared by a photo-deposition method. The photocatalytic properties of the prepared Pt/TiO_2 foam nickel were investigated.

The photocatalytic activities of all the samples were evaluated by photocatalytic degradation efficiency of gaseous acetaldehyde, which is used as a representative of indoor volatile organic compounds (VOCs). The promotion effects of Al_2O_3–SiO_2 film as transition layer and Pt loading on TiO_2/nickel-foam catalyst are investigated. The effects of photocatalyst preparation parameters along with their photocatalytic behavior in deactivation and reactivation are also presented in the present study.

2. Experimental

2.1. Preparation of samples

All chemicals were of analytical grade, provided by China Medicine (Group) Shanghai Chemical Reagent Corporation Limited. Precursor solutions for Al_2O_3–SiO_2, TiO_2 and TiO_2/Al_2O_3–SiO_2 films were prepared via sol–gel processes. The corresponding sols were prepared as follows. Aluminum chloride hexahydrate ($AlCl_3{\cdot}6H_2O$, 24.145 g), anhydrous ethanol (116.6 ml) and ethyl silicate (TEOS, 7.467 ml) were added into a flask connected with a reflex condenser. The resultant mixture was kept boiling at 60 °C and refluxing until the aluminum chloride hexahydrate was dissolved under vigorous stirring, then a uniform, stable, and transparent sol of Al_2O_3–SiO_2 was obtained. The molar ratio of Al_2O_3 and SiO_2 is 3:2. A detailed description of the TiO_2 sol preparation is given elsewhere [19].

In the preparation of TiO_2 or Al_2O_3–SiO_2 films, the substrate foam nickel was rinsed with acetone and then washed thoroughly with deionized water. A piece of pre-dried foam nickel was dipped in the Al_2O_3–SiO_2 sol for minutes and then rotated at high speed to form a wet gel film. After drying at room temperature for 12 h, the sample was calcined at 550 °C in an air-flow oven for 45 min. TiO_2 films were deposited according to the same procedure and calcined at 550 °C for 1 h. When Al_2O_3–SiO_2 films act as interlayer, TiO_2 is coated on Al_2O_3–SiO_2 films other than on foam metal nickel.

The operations of dipping, drying and heating in air were repeated several times in order to obtain Al_2O_3–SiO_2 films coated on foam nickel and subsequently TiO_2 films on Al_2O_3–SiO_2 layer with various coating cycles. The prepared samples will be denoted as AS1, AS2, AS1T1, AS2T2, where T and AS indicate TiO_2 and Al_2O_3–SiO_2 respectively, and the numbers followed indicate the coating cycles of the films. The arranged order of T and S expresses the deposition order of TiO_2 and Al_2O_3–SiO_2 films.

Platinized TiO_2 films were prepared by a photo-deposition method. The TiO_2 or TiO_2/Al_2O_3–SiO_2-loaded foam nickel was immersed in aqueous solution of hexachloroplatinic acid ($H_2PtCl_6{\cdot}6H_2O$). The concentration of the solution changes to insure the Pt loading on TiO_2 is from 0.2 wt% to 0.4 wt%. Irradiation was carried out using a 300 W Xe lamp for 3 h to evaporate the solution entirely. After irradiation, Pt–TiO_2 or Pt–TiO_2/Al_2O_3–SiO_2 was washed thoroughly with deionized water and dried at 100 °C for 4 h in an oven.

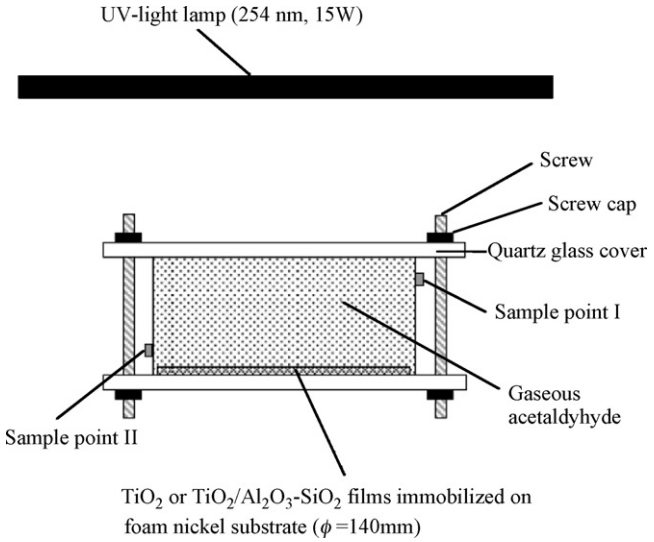

Fig. 1. Schematic diagram of photoreactor for acetaldehyde photocatalytic degradation.

2.2. Characterization

The X-ray diffraction (XRD) patterns were identified by an X-ray diffractometer (Bruker, D8 ADVANCE) with Cu Kα radiation (λ = 1.5405 Å) operated at 40 kV and 40 mA. The SSAs were measured by nitrogen adsorption by BET method (Quantachrome Instruments, NOVA 1000). The ultraviolet–visible (UV–vis) absorption spectra of the films were recorded on a TU 1901 UV–vis spectrophotometer (Beijing Purkinje General Instrument Co. Ltd.). Photoluminescence emission spectra were recorded by LS-50B (PerkinElmer Co., US).

2.3. Evaluation of photocatalytic activity

The photocatalytic activities of samples were evaluated by photocatalytic degradation of gaseous acetaldehyde. The TiO_2-, TiO_2/Al_2O_3–SiO_2-, or Pt–TiO_2/Al_2O_3–SiO_2-coated foam nickel (ϕ = 140 mm) was put on the bottom of a cylindrical reactor, which was provided with a quartz window of ca. 167.3 cm^2 and a volume of 1000 cm^3 (Fig. 1). The bare foam nickel without any loading and foam nickel loaded with only Al_2O_3–SiO_2 films were used for blank tests. Gaseous acetaldehyde (from Guang Ming Special Gas Co. Ltd., Dalian) was injected into the reactor. The initial concentration of acetaldehyde injected into the reactor was ca. 100 ppmv. The irradiation was started after the equilibrium between gaseous and adsorbed acetaldehyde was reached using a UV lamp (main wavelength λ_{main} = 253.7 nm; 15 W) through the quartz window. The vertical distance between light source and photocatalyst was 25 cm. The concentrations of acetaldehyde and CO_2 in gas phase were measured by a gas chromatograph (GC9160-HA, Haixin Co. Ltd., Shanghai) equipped with a flame ionization detector (FID) and a methanizer operated at 350 °C. The removal ratio of acetaldehyde was calculated from the amount of CO_2 evolution.

3. Results and discussion

3.1. Promotion effect of Al_2O_3–SiO_2 interlayer

Fig. 2 shows XRD patterns of samples AS2 and AST2. The diffraction peaks are assigned to anatase TiO_2, NiO and Ni. NiO comes from the partial oxidation of metal Ni during heat treatment. No characteristic diffraction peaks attributed to $3Al_2O_3{\cdot}2SiO_2$ are

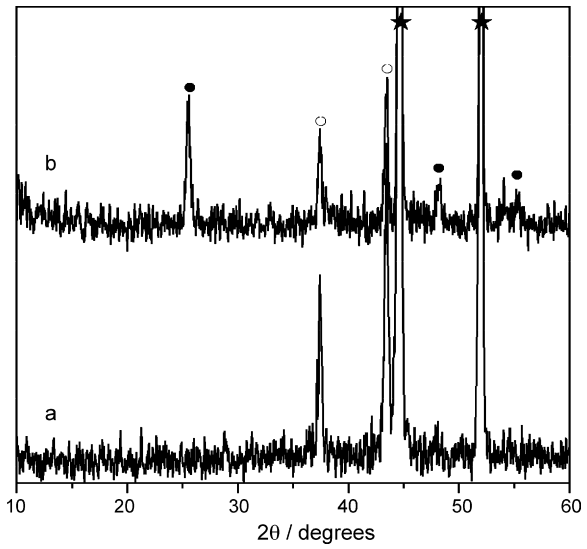

Fig. 2. XRD patterns of AS2 (a) and AS2T2 (b) films loaded on foam nickel (symbol—●: anatase TiO_2, ○: NiO, ★: Ni).

observed. It indicates that Al_2O_3–SiO_2 interlayer between TiO_2 film and the Ni substrate did not crystallize under the calcination temperature and might keep amorphous state. Usually, the complete crystallization of silicate $3Al_2O_3{\cdot}2SiO_2$ should be heat-treated up to 1200 °C. In this experiment condition, the uncondensed Al_2O_3–SiO_2 interlayer may possess higher specific surface area. It is conformed by the measurement of SSA in Fig. 3.

Fig. 3 shows the nitrogen adsorption–desorption curves and the pore size distribution calculated from desorption isotherms of Al_2O_3–SiO_2 powder prepared by sol–gel method. The Al_2O_3–SiO_2 powder has high SSA of 117.6 $m^2\,g^{-1}$. The pore size distribution is very concentrated with an average size of 5 nm, belonging to mesoporous materials. The measured SSAs of sample TiO_2, AS1T1, AS1T2, AS2T1 and AS2T2 films are 0.7 $m^2\,g^{-1}$, 20.3 $m^2\,g^{-1}$, 26.7 $m^2\,g^{-1}$, 24.6 $m^2\,g^{-1}$ and 28.5 $m^2\,g^{-1}$, respectively. It was found that the increase of dip-coating cycles resulted in the weight increase of either AS coating or further TiO_2 coating on AS layer. The weight increase percentage and the relevant SSAs of samples are summarized in Table 1. The Al_2O_3–SiO_2 film loaded on foam nickel as transition layer contributes greatly to provide higher SSA for photocatalyst-loading on substrate, resulting in more active sites.

The UV–vis absorption spectra of the prepared TiO_2 and Al_2O_3–SiO_2 powder are shown in Fig. 4. Al_2O_3–SiO_2 powder has little absorption in UV region, which indicating that the introduction of Al_2O_3–SiO_2 interlayer has almost no impairment to the photo-absorption and exciting for TiO_2 photocatalyst.

The degradation ratios of gaseous acetaldehyde were calculated according to the equation:

$$R_t = \frac{C_t}{C_i} \quad (1)$$

where R_t is the degradation ratio of gaseous acetaldehyde, C_i denotes the initial concentration of gaseous acetaldehyde

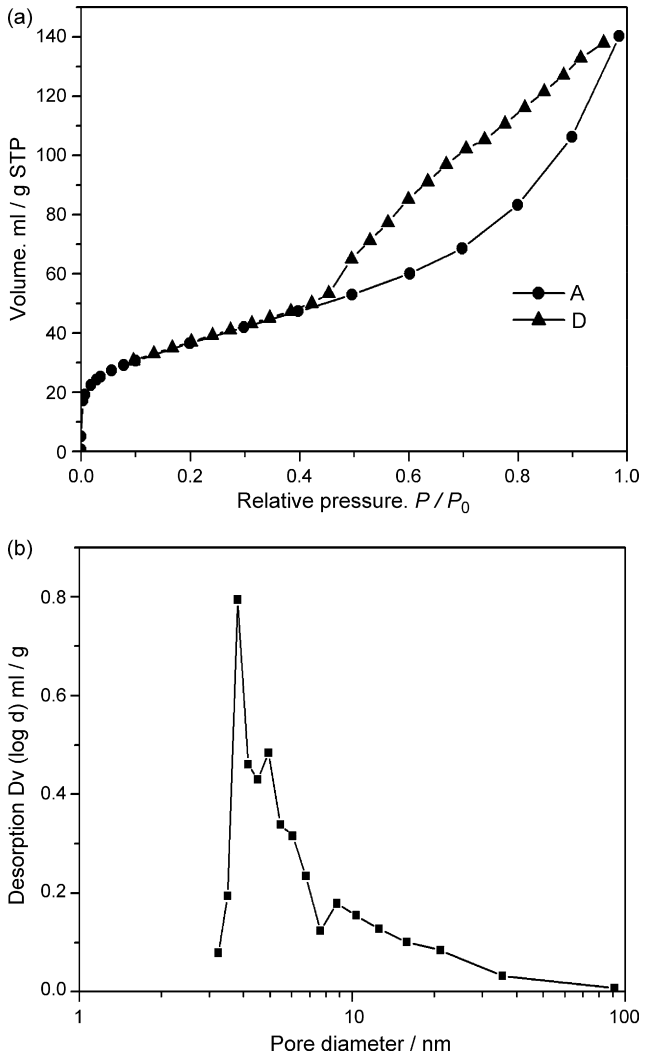

Fig. 3. N_2 adsorption–desorption isotherms curve (a) and pore size distribution (b) of Al_2O_3–SiO_2 powder obtained from sol–gel method.

(100 ppmv) and C_t is the concentration of completely decomposed acetaldehyde during the reaction calculated from the amount of CO_2 evolution (the complete photocatalytic decomposition of one acetaldehyde molecule yields two carbon dioxide molecules) measured by a gas chromatograph.

Comparison reactions were performed in the dark or without TiO_2 (i.e., using the substrate samples) under the same experimental conditions of the irradiation experiments. There was no degradation of acetaldehyde be observed in the absence of TiO_2 even under UV light irradiation.

Fig. 5 presents the photocatalytic decomposition of gaseous acetaldehyde on AST films immobilized on foam nickel under UV light irradiation. The removal ratios of gaseous acetaldehyde increased obviously compared to that of TiO_2 [19]. The photocatalytic decomposition of acetaldehyde reached almost 100% in

Table 1
Experimental data of TiO_2/Al_2O_3–SiO_2 photocatalysts coated on foam nickel

Samples	SSAs of AS on Ni-foam ($m^2\,g^{-1}$)	Weight increase of TiO_2 (%)	SSAs of AST on Ni-foam ($m^2\,g^{-1}$)	Acetaldehyde-removal percent in 90 min (%)
AS1T1	87.6	4.7	20.3	44
AS1T2	87.6	8.6	26.7	78
AS2T1	94.7	4.3	24.6	39
AS2T2	94.7	9.1	28.5	93

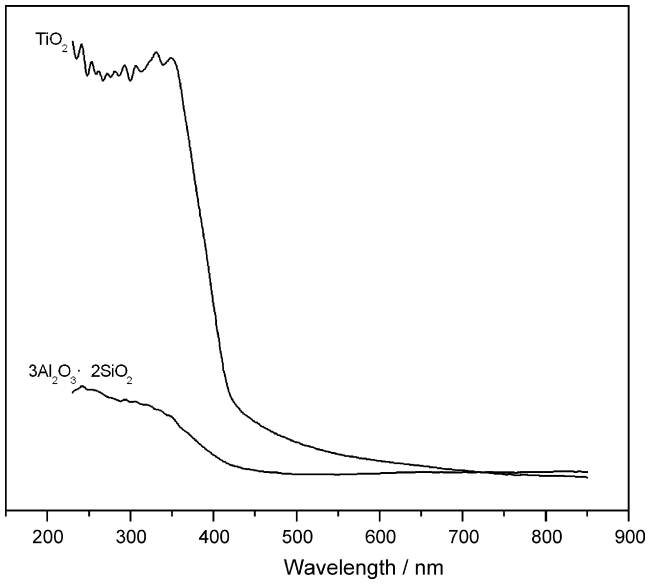

Fig. 4. UV–vis absorption spectra of TiO_2 and Al_2O_3–SiO_2 powders.

120 min on AS2T2, while the removal rate on TiO_2 films without interlayer is only about 40% [19]. Furthermore, as shown in Table 1, the photocatalytic activity of complete oxidation for total acetaldehyde shows the following order: AS2T2 > AS1T2 > AS1T1 > AS2T1. The photocatalytic activity order for AS1T1 > AS2T1 may be attributed to the higher content of loaded TiO_2 for AS1T1 even though the SSAs of AS1T1 are lower than that of AS2T1.

Deactivation of photocatalyst is a very common problem encountered in practice. It arises from the accumulation of photocatalytic reaction intermediates and final products on catalyst surface [24,25]. In order to evaluate the photocatalytic stability of TiO_2 and AST films, consecutive degradation reactions of gaseous acetaldehyde were carried out. As shown in Fig. 6, the photocatalytic activities of both T2 and AS2T2 films decreased gradually in subsequent runs. However, the deactivation of AS2T2 is rather slower than that of T2. Nevertheless, the complete reactivations of T2 and AS2T2 films are achieved by heating them at 300 °C for 1 h. No visible deactivation caused by the exfoliation of photocatalyst during the reactions was observed. The adhesion properties of the prepared films on foam nickel wafer are good

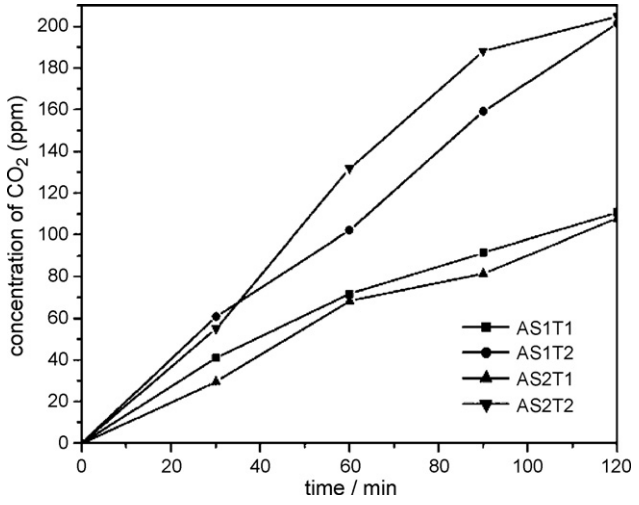

Fig. 5. Gaseous acetaldehyde degradation rates of various AST films coated on foam nickel (light source: UV lamp, λ_{main} = 253.7 nm, 15 W).

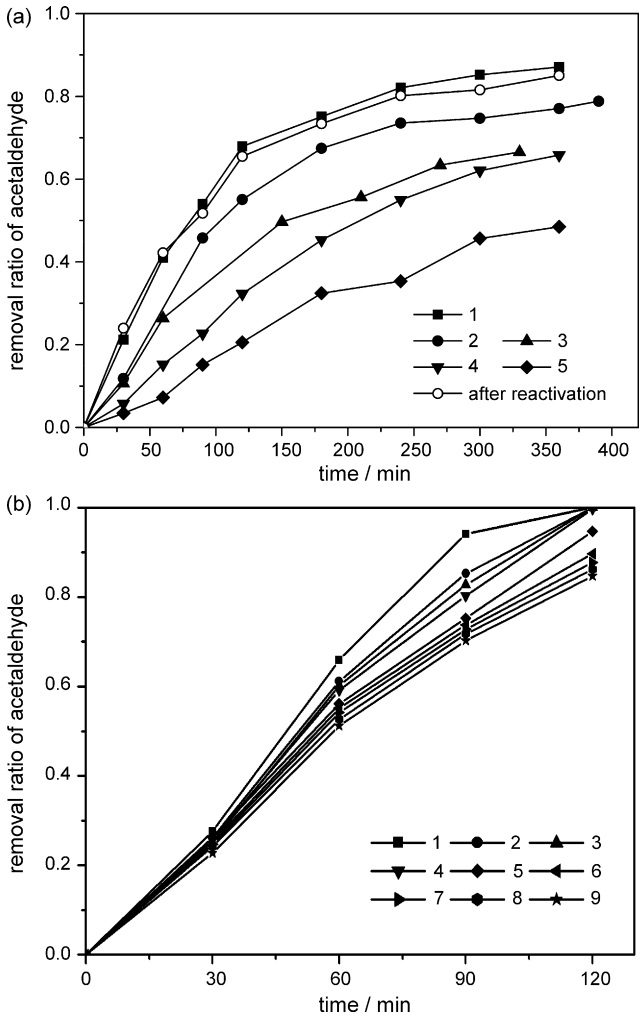

Fig. 6. Time course of the CO_2 concentration produced by CH_3CHO photodecomposition on TiO_2 films (a) and AS_2T_2 films (b) with several consecutive runs (light source: UV lamp, λ_{main} = 253.7 nm, 15 W). Reactivation was conducted by heating at 300 °C for 1 h.

enough for application. All of AST samples have no photocatalytic activity under visible light irradiation.

It is apparent that the Al_2O_3–SiO_2 interlayer helped to increase photo-degradation rate of acetaldehyde and modified deactivation of TiO_2 on foam nickel substrate. The promotion effect attributed to the high SSA of Al_2O_3–SiO_2 interlayer, which provides more active sites for photocatalytic reaction. Similar to NiO [19], the inert Al_2O_3–SiO_2 interlayer prevented effectively the transfer of photogenerated electrons from TiO_2 films to metal Ni, resulting in the promotion of photocatalytic reaction.

3.2. Promotion effect of Pt loading

Fig. 7 shows the comparison of XRD patterns of TiO_2 and Pt–TiO_2 powder (denoted as GPT, the following numbers 02, 03 and 04 represent the Pt loading wt% 0.2 wt%, 0.3 wt% and 0.4 wt%, respectively). There are no observational changes occurred for the peaks of anatase TiO_2, and also no diffraction peaks assigned to Pt. It means that Pt loading did not result in the crystalline phase transformation of TiO_2. Pt-deposition was in high dispersion and low concentration. Fig. 8 shows the UV–vis absorption spectra of TiO_2 powders with and without Pt loading. It is clear that Pt loading in the range of 0.2–0.4 wt% did not reduce the transmittance in the

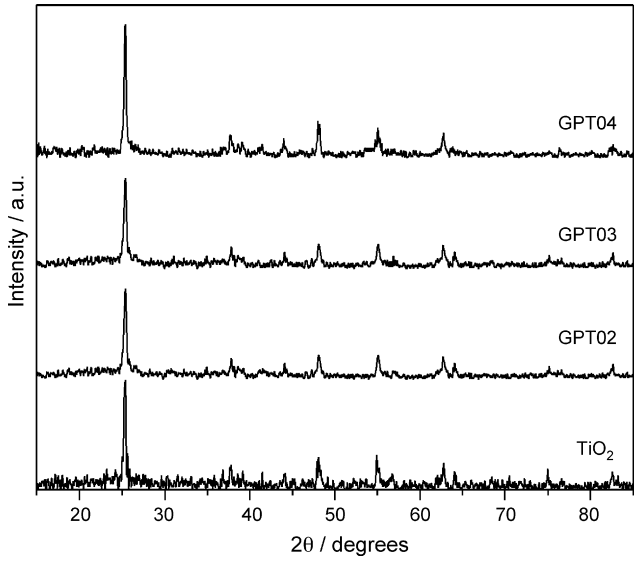

Fig. 7. XRD patterns of TiO_2 powder and Pt–TiO_2 powders prepared by photo-deposition.

entire wavelength range, indicating that the Pt loading amount is quite small. From the FE–SEM image of Pt–TiO_2 films coated on foam nickel in Fig. 9, it is found that Pt dispersed homogeneously with spherical particles of about the size of 40–100 nm agglomerated by finer primary particles of about 10 nm, which is crucial to obtain higher photocatalytic efficiency. This kind of nano-sized particles might not be found in samples without Pt loading. Fig. 10 shows the photocatalytic activities of various Pt–TiO_2 films coated on foam nickel for the degradation of gaseous acetaldehyde under UV illumination. The removal ratio reaches 100% in 70 min for the samples with 0.2 wt% and 0.3 wt% Pt loading TiO_2, being as more than three times as that of TiO_2 without Pt. When the amount of Pt loading exceeds 0.3 wt%, the activity of Pt–TiO_2 decreases slightly.

It has widely been believed that Schottky barrier is formed when Pt contacts with TiO_2 [26–28]. The photo-excited electrons under irradiation flow from TiO_2 to platinum. Platinum with high electron affinity, acts as an electron sink, retards the recombination of the charge carriers (i.e., electrons and holes), thus enhancing the

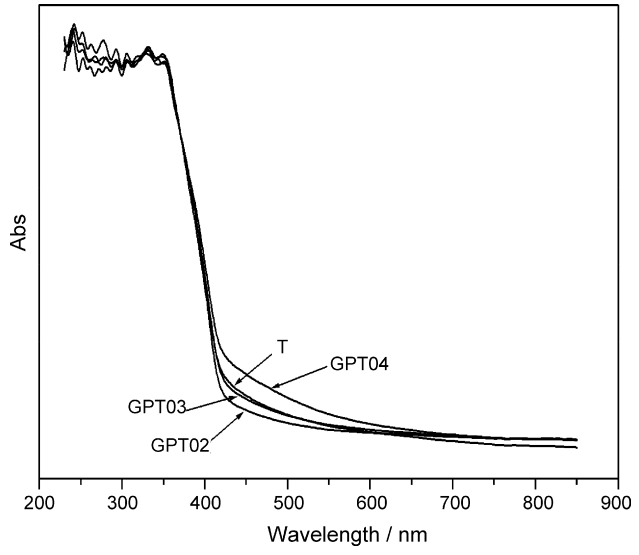

Fig. 8. UV–vis absorption spectra of TiO_2 and Pt–TiO_2 powders prepared by photo-deposition.

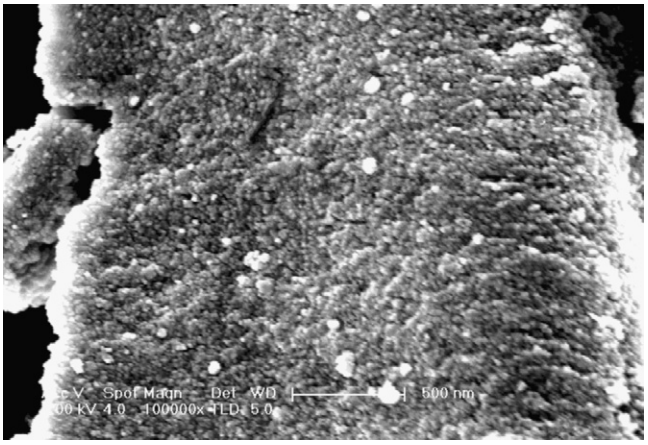

Fig. 9. FE–SEM image of Pt/TiO_2 films coated on foam nickel prepared by photo-deposition method.

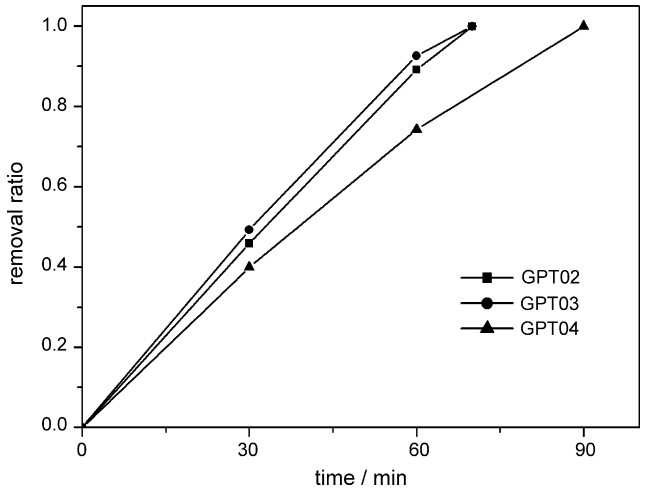

Fig. 10. Gaseous acetaldehyde degradation rates of various Pt–TiO_2 films coated on foam nickel prepared by photo-deposition method (light source: UV lamp, λ_{main} = 253.7 nm, 15 W).

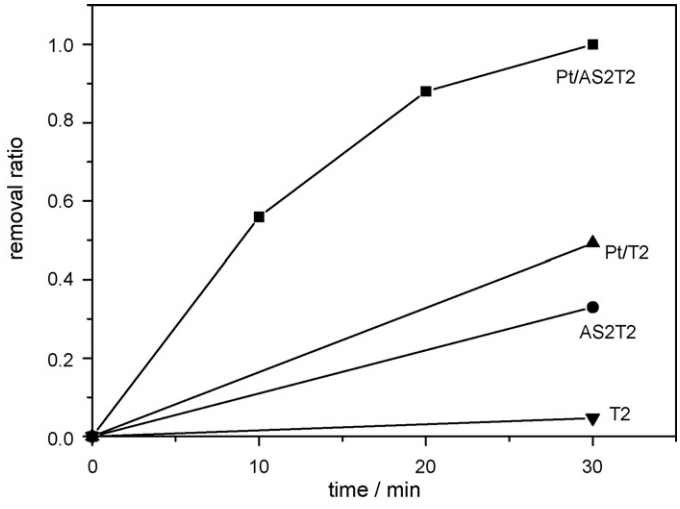

Fig. 11. Gaseous acetaldehyde degradation rates of S2T2 and T1 films coated on foam nickel substrate without Pt deposition and with 0.3 wt% of Pt deposited by photo-deposition (light source: UV bactericide lamp, λ_{main} = 253.7 nm, 15 W).

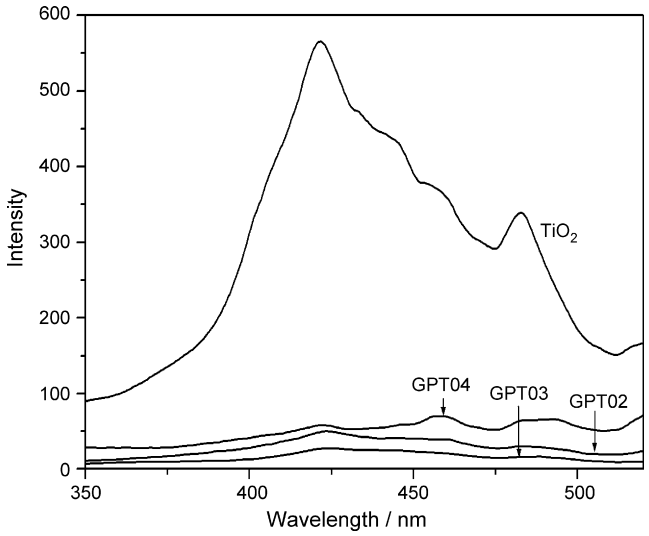

Fig. 12. Photoluminescence emission spectra of TiO_2 and Pt–TiO_2 powders prepared by photo-deposition method (excitation: 360 nm).

photoactivity. Fig. 11 presents the gaseous acetaldehyde degradation rates of S2T2 and T1 films coated on foam nickel substrate without Pt deposition and with 0.3 wt% of Pt deposited by photo-deposition. Apparently, loading of Pt improves the photoactivity greatly as expected. In an effort to understand the role of Pt in photocatalytic reactions, photoluminescence emission spectra of TiO_2 and Pt–TiO_2 powders is shown in Fig. 12. The PL intensity of the entire Pt loading TiO_2 is much lower than that of TiO_2, conforming the retardation of Pt to the recombination of photo-generated electrons and holes. When deposited on TiO_2 excessively, Pt probably becomes the recombination sites of photo-generated electrons and holes, and then the recombination rate will increase. At the same time, the over-deposited metal Pt blocks the UV light irradiation and reduces the number of photo-generated electrons and holes on photocatalyst. As a result, the photocatalytic activity is depressed. In this study, the highest photocatalytic activity of Pt–TiO_2 is obtained by 0.3 wt% deposition of Pt.

4. Conclusions

TiO_2 photocatalysts coated on foam nickel were prepared by sol–gel method, and Al_2O_3–SiO_2 films were successfully introduced as interlayer between TiO_2 and foam nickel substrate via sol–gel approach. The interlayer remarkably enhanced active sites for photocatalytic reaction by providing large SSA for TiO_2 loading, resulting in higher photocatalytic activity and stability of TiO_2 photocatalyst. It is indicated that the use of the SiO_2–Al_2O_3 interlayer on TiO_2/nickel-foam is a favorable approach to the commercial application of photocatalysts for the effective removal of volatile organic compounds. At the same time, chemical inert Al_2O_3–SiO_2 prevented the transfer of photo-generated electron from TiO_2 to metal Ni, and then promoted the photocatalytic activity. Furthermore, Pt loading increases the photoactivity as more than three times as that of TiO_2 (or TiO_2 with Al_2O_3–SiO_2 interlayer). Pt acts as an electron sink to retard the recombination of the charge carriers and thus enhancing the photoactivity. The optimum Pt loading is about 0.3 wt%.

Acknowledgments

The study was supported by The Special Foundation of Nanometer Technology (No. 0552nm002, No. 0752nm005) from Shanghai Municipal Science and Technology Commission (STCSM) and National Basic Research Program of China (973 Program) No. 2007CB613305.

References

[1] D.A. Tryk, A. Fujishima, K. Honda, Electrochim. Acta 45 (2000) 2363.
[2] W. Bahnemann, M. Muneer, M.M. Haque, Catal. Today 124 (3–4) (2007) 133.
[3] M.R. Hoffmann, S.T. Martin, W. Choi, D.W. Bahnemann, Chem. Rev. 95 (1) (1995) 69.
[4] M.A. Fox, M.T. Dulay, Chem. Rev. 93 (1) (1993) 341.
[5] H.S. Hafez, A.E.H. Ali, M.S.A. Abdel-Mottaleb, Int. J. Photoenergy 7 (4) (2005) 181.
[6] J.C. Yu, J.G. Yu, L.Z. Zhang, W.K. Ho, J. Photochem. Photobiol. A: Chem. 148 (2002) 263.
[7] I. Sopyan, M. Watanabe, S. Murasawa, K. Hashimoto, A. Fujishima, J. Electroanal. 415 (1996) 183.
[8] W.D. Sproul, M.E. Graham, M.S. Wong, P.J. Rudnik, Surf. Coat. Technol. 89 (1997) 10.
[9] Q.M. Zhang, G.L. Griffin, Thin Solid Films 263 (1995) 65.
[10] J.G. Yu, X.J. Zhao, Q.N. Zhao, Thin Solid Films 379 (2000) 7.
[11] J.T. Richardson, M. Garrait, J.K. Hung, Appl. Catal. A 255 (2003) 69.
[12] Y. Peng, J.T. Richardson, Appl. Catal. A 266 (2004) 235.
[13] F.C. Buciuman, B.K. Czarnetzki, Catal. Today 69 (2001) 337.
[14] K.S. Hwang, H.Y. Zhu, G.Q. Lu, Catal. Today 68 (2001) 183.
[15] Z. Ding, X.J. Hu, P.L. Yue, G.Q. Lu, P.F. Greenfield, Catal. Today 68 (2001) 173.
[16] A.I. Molina, J.M. Robles, P.B. García, E.R. Castellon, E. Finocchio, G. Busca, P.M. Torres, A.J. Lopez, J. Catal. 225 (2004) 479.
[17] P. Atienzar, A. Corma, H. Garcia, J.C. Scaiano, Chem. Mater. 16 (2004) 982.
[18] F.L.Y. Lam, X.J. Hu, Chem. Eng. Sci. 58 (2003) 687.
[19] H. Hu, W.J. Xiao, J. Yuan, J.W. Shi, M.X. Chen, W.F. Shangguan, J. Environ. Sci. 19 (2007) 80.
[20] W.K. Wong, M.A. Malati, Sol. Energy 2 (1986) 163.
[21] A. Davidson, M. Che, J. Phys. Chem. 96 (1992) 9909.
[22] K.T. Ranjit, B. Viswanathan, J. Photochem. Photobiol. A: Chem. 107 (1997) 215.
[23] K.T. Ranjit, B. Viswanathan, J. Photochem. Photobiol. A: Chem. 108 (1997) 73.
[24] M.L. Sauer, D.F. Ollis, J. Catal. 163 (1996) 215.
[25] J. Peral, D.F. Ollis, J. Mol. Catal. A: Chem. 115 (1997) 347.
[26] B.Y. Lee, S.H. Park, S.C. Lee, M. Kang, C.H. Park, S.J. Choung, Korean J. Chem. Eng. 20 (2003) 812.
[27] T. Sakata, T. Kawai, K. Hashimoto, Chem. Phys. Lett. 88 (1982) 50.
[28] K.D. Schierbaum, S. Fischer, P. Wincott, P. Hardman, V. Dhanak, G. Jones, G. Thornton, Surf. Sci. 391 (1997) 196.